

Valley-optronics of impurity states in two-dimensional Dirac materials

Dogyun Ko,^{1,2} A. V. Morozov,³ V. M. Kovalev,^{3,4} and I. G. Savenko^{1,2}

¹*Center for Theoretical Physics of Complex Systems,
Institute for Basic Science (IBS), Daejeon 34126, Korea*

²*Basic Science Program, Korea University of Science and Technology (UST), Daejeon 34113, Korea*

³*Rzhanov Institute of Semiconductor Physics, Siberian Branch,
Russian Academy of Sciences, Novosibirsk, 630090 Russia*

⁴*Department of Applied and Theoretical Physics,
Novosibirsk State Technical University, Novosibirsk 630073, Russia*

(Dated: April 1, 2025)

We analyze the valley selection rules for optical transitions from impurity states to the conduction band in two-dimensional Dirac materials, taking a monolayer of MoS₂ as an example. We employ the analytical model of a shallow impurity potential which localizes electrons described by a spinor wave function, and, first, find the system eigenstates taking into account the presence of two valleys in the Brillouin zone. Then, we find the spectrum of the absorbance and calculate the photon-drag electric current due to the impurity-band transitions, drawing the general conclusions regarding the valley optical selection rules for the impurity-band optical transitions in gapped Dirac materials.

The key idea of valleytronics is in using the valley index as an additional active degree of freedom of charge carriers [1, 2] in gapped graphene [1], monolayers of transition metal dichalcogenides (TMDs) [2], among other two-dimensional (2D) Dirac materials. One of the representatives of TMDs is MoS₂: a material with a structure composed of molybdenum atoms sandwiched between pairs of sulfur atoms. In contrast to graphene, it is characterized by the inversion symmetry breaking and it possesses a large band gap with the width in the optical range, absent in monolayer graphene [3]. It represents a direct band gap material with the minima of the conduction band and maxima of the valence band located at points K and K' in reciprocal space. Moreover, electrons in MoS₂ are subject to strong spin-orbital interaction, which also makes it different from graphene, where the spin-orbital interaction is relatively weak. This latter property, which is due to the electrons occupying d-orbitals in MoS₂, results in an extra band splitting [4].

It has been shown that the interband (between the conduction and valence bands) transitions in Dirac materials are valley-sensitive: at a given circular polarization of the external electromagnetic perturbation, the interband transitions occur predominantly in one valley since the electrons in each valley couple with a specific polarization of light [5]. Switching to the opposite circular polarization changes the valley where the interband transitions take place [6]. These optical selection rules are fulfilled exactly for interband optical transitions, where the electron momentum is a good quantum number.

However, each material is to some extent disordered: it contains impurities, some of which are unintentional and emerge due to the imperfections of the growth technique, whereas some of the impurities are embedded intentionally in order to enhance electronic (or other) properties of the sample. As a result, there emerge additional donor and acceptor energy levels in the vicinity of the conduction and valence bands, respectively. Then, if the sample is exposed to external light with the frequency smaller

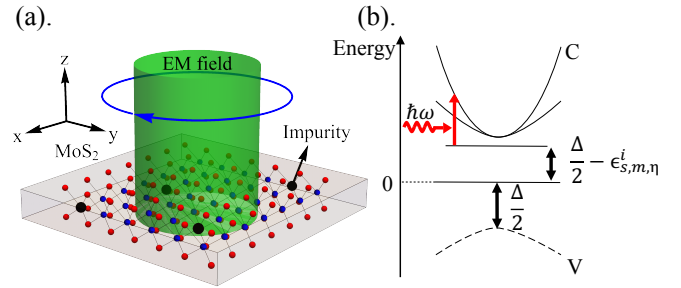


FIG. 1. System schematic. (a) A monolayer of MoS₂ (with impurities) exposed to a circularly polarized electromagnetic (EM) field of light (green cylinder). (b) The bandstructure of MoS₂. The band gap is Δ , and the system is exposed to an EM field with frequency ω .

than the band gap of the material, the optical properties become mostly determined by the electron transitions from donor impurities to the conduction band and from the valence band to the acceptor states [7]. In this case, the electron states on impurities are characterized by some quantum numbers instead of the translational momentum due to localization. The theoretical description of optical transitions from these states to the bands and the analysis of the corresponding optical selection rules, which take into account the valley quantum number, represents an important problem of valley optoelectronics, and it has been studied theoretically. In particular, work [8] presents a numerical study of a special type of disorder: the vacancy defects.

It is also important to know the general properties of defects of any type, and an analytical analysis would be beneficial. However, one of the problems here is that the simple model, which assumes the impurity potential energy to be the Dirac delta-function [9], is not applicable in the case of a Dirac Hamiltonian since the electron wave function becomes singular exactly at the center of coordinates. But this latter problem has found its (semi-

analytical) solution [10]. In this paper, we build a theory of impurity-band transitions in 2D Dirac materials, utilizing and modifying the model of zero-radius impurity potential, which is frequently used for the description of shallow impurities in semiconductors and semiconductor nanostructures [10, 11]. We investigate the optical properties of disordered TMDs, examining the light absorption and photoinduced transport effects, accounting for the spin-orbital coupling of electrons. We study the behavior of drag electric current density and the absorption coefficient for different key parameters of the sample and different polarizations of the incident light.

Hamiltonian and eigenstates. The light absorption is governed by microscopic transitions of electrons from the bound impurity states to the conduction band. The Hamiltonian of the electron bound at the attractive potential $u(\mathbf{r})$ reads

$$H = \left(\frac{\Delta}{2} \sigma_z + \mathbf{v} \mathbf{p} \right) \otimes \mathbb{1} - \frac{\lambda \eta}{2} (\sigma_z - \mathbb{1}) \otimes \hat{s}_z + u(\mathbf{r}), \quad (1)$$

where Δ is a band gap, $\mathbf{v} = v(\eta \sigma_x, \sigma_y)$ is the velocity operator, \mathbf{p} is the electron momentum, and σ_α with $\alpha = x, y, z$ the Pauli matrices of pseudospin. The index $\eta = \pm 1$ indicates the valley; λ is intrinsic spin-orbital coupling; \hat{s}_z is the matrix of the electron spin. The first term in Hamiltonian (1) describes a two-band model of gapped graphene (or a band structure of a TMD material). We consider a shallow impurity potential, $u(\mathbf{r})$, thus we assume that the ionization potential of the donor is much smaller than Δ .

To find the eigenfunctions and eigenenergies, we write the Schrödinger equation in the momentum representation,

$$\begin{pmatrix} \frac{\Delta}{2} - E & vp_- \\ vp_+ & -\frac{\Delta}{2} + s\lambda\eta - E \end{pmatrix} \chi_{s,m}(\mathbf{p}) + \int \frac{d\mathbf{p}'}{(2\pi\hbar)^2} u(\mathbf{p} - \mathbf{p}') \chi_{s,m}(\mathbf{p}') = 0, \quad (2)$$

where $s = \pm 1$, $p_\pm = \eta p_x \pm ip_y = pe^{\pm i\eta\varphi}$ with φ the angle of the vector \mathbf{p} with respect to x -axis, m is the eigenvalue of the z -projection of the electron angular momentum (the quantum number which characterizes electron localized on impurity),

$$\begin{aligned} u(\mathbf{p} - \mathbf{p}') &= 2\pi \int_0^\infty r dr u(r) J_0(|\mathbf{p} - \mathbf{p}'|r) \\ &= 2\pi \sum_k \int_0^\infty r dr u(r) J_k(pr) J_k(p'r) \cos k(\varphi - \varphi'), \end{aligned} \quad (3)$$

where $J_k(x)$ are the k -order Bessel functions. We search for the spinor eigenfunctions in the form,

$$\chi_{s,m}(\mathbf{p}) = \begin{pmatrix} a_{s,m}(p) e^{im\varphi} \\ b_{s,m}(p) e^{i(m+\eta)\varphi} \end{pmatrix} \quad (4)$$

since this form reflects the axial symmetry, and the eigenstates are characterized by the angular momentum projection with quantum number m . Substituting Eq. (4)

in Eq. (2) and performing the integration over φ' we find the system of equations for the coefficients $a_{s,m}$ and $b_{s,m}$,

$$\begin{aligned} 0 &= \begin{pmatrix} \frac{\Delta}{2} - E & vp \\ vp & -\frac{\Delta}{2} + s\lambda\eta - E \end{pmatrix} \begin{pmatrix} a_{s,m}(p) \\ b_{s,m}(p) \end{pmatrix} \\ &+ \int_0^\infty r dr u(r) \int_0^\infty \frac{p' dp'}{\hbar^2} \begin{pmatrix} J_m(pr) J_m(p'r) a_{s,m}(p') \\ J_{(m+\eta)}(pr) J_{(m+\eta)}(p'r) b_{s,m}(p') \end{pmatrix}. \end{aligned} \quad (5)$$

To draw principal conclusions, we can now simplify these equations. For a shallow impurities ($\epsilon_{s,m,\eta}^i \ll \Delta$) and low enough temperatures only the low-lying impurity states are occupied. Then, we can consider the transitions from impurity states corresponding to $m = 0$ and $m = \pm 1$ levels. Assuming that the potential of each impurity $u(r)$ is sharply peaked in the vicinity of its center $r = 0$ and it rapidly decreases with r , we can take the Bessel functions under the integral at $r = 0$. For the $m = 0$ state, $J_0(0) = 1$ and $J_{\eta=\pm 1}(0) = 0$, and we find the simplified form of Eq. (5),

$$\begin{pmatrix} \epsilon_{s,0,\eta}^i & vp \\ vp & -\Delta + s\lambda\eta \end{pmatrix} \begin{pmatrix} a_{s,0} \\ b_{s,0} \end{pmatrix} + \begin{pmatrix} Au_0 \\ 0 \end{pmatrix} = 0, \quad (6)$$

where

$$A = \int_0^\infty \frac{p' dp'}{\hbar^2} a_{s,0}(p'); \quad u_0 = \int_0^\infty u(r) r dr. \quad (7)$$

The solution reads

$$\begin{pmatrix} a_{s,0} \\ b_{s,0} \end{pmatrix} = -\hbar v \sqrt{\frac{2\pi\epsilon_{s,0,\eta}^i}{\Delta}} \begin{pmatrix} \frac{\Delta - s\lambda\eta}{(vp)^2 + \epsilon_{s,0,\eta}^i(\Delta - s\lambda\eta)} \\ \frac{vp}{(vp)^2 + \epsilon_{s,0,\eta}^i(\Delta - s\lambda\eta)} \end{pmatrix}. \quad (8)$$

For the $m = 1, \eta = -1$ state, $J_0(0) = 1$, $J_1(0) = 0$, and $J_2(0) = 0$, Eq. (5) can be simplified,

$$\begin{pmatrix} \epsilon_{s,1,-1}^i & vp \\ vp & -\Delta - s\lambda \end{pmatrix} \begin{pmatrix} a_{s,1} \\ b_{s,1} \end{pmatrix} + \begin{pmatrix} 0 \\ Bu_0 \end{pmatrix} = 0, \quad (9)$$

where now

$$B = \int_0^\infty \frac{p' dp'}{\hbar^2} b_{s,1}(p'). \quad (10)$$

The solution of (9) reads

$$\begin{pmatrix} a_{s,1} \\ b_{s,1} \end{pmatrix} = -\hbar v \sqrt{\frac{2\pi(\Delta^2 - \lambda^2)}{\Delta\epsilon_{s,1,-1}^i}} \begin{pmatrix} \frac{vp}{(vp)^2 + \epsilon_{s,1,-1}^i(\Delta + s\lambda)} \\ \frac{-\epsilon_{s,1,-1}^i}{(vp)^2 + \epsilon_{s,1,-1}^i(\Delta + s\lambda)} \end{pmatrix}. \quad (11)$$

The energy $\epsilon_{s,1,-1}^i$ of this state can be also found using the definition Eq. (10). We see that within the framework of the shallow-impurity model, the state $m = 1$ forms ‘under’ the $\eta = -1$ valley (and vice versa). In other words, the following rule holds: $m + \eta = 0$ for $m = \pm 1$ states.

The electron states in the conduction band are described by the wave function,

$$\psi_{s,\eta}(\mathbf{p}) = \begin{pmatrix} \cos\left(\frac{\theta_{s,\eta}}{2}\right) \\ \sin\left(\frac{\theta_{s,\eta}}{2}\right) e^{i\eta\varphi_{\mathbf{p}}} \end{pmatrix} \quad (12)$$

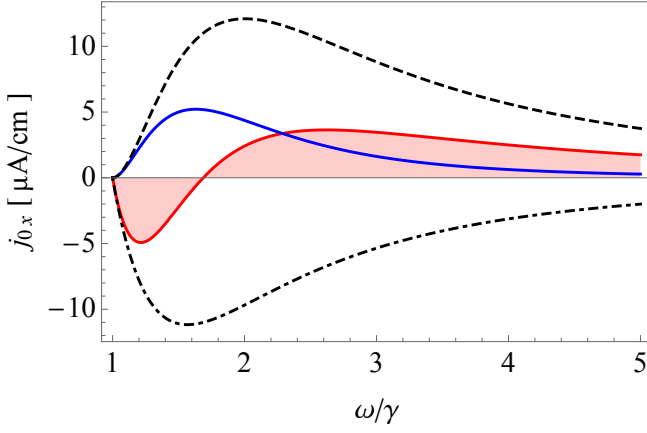


FIG. 2. Spectrum of electric current density due to the transitions from $m = 0$, $\eta = -1$ impurity states to spin-up conduction band states for the polarization of light $\sigma = -1$ (red) and $\sigma = 1$ (blue); $\gamma = \epsilon_{1,0,-1}^i/\hbar$, where $\epsilon_{1,0,-1}^i = 10$ meV is the energy of impurity counted from the bottom of the conduction band. Black curves show the positive and negative contributions to current in $\sigma = -1$ case. We used the density of impurities $n_i \approx 5 \times 10^{12} \text{ cm}^{-2}$; electron relaxation time $\tau = 2 \times 10^{-13} \text{ s}$, velocity $v = at/\hbar$, the lattice constant of MoS₂ $a = 3.193 \text{ \AA}$, effective hopping integral $t = 1.10 \text{ eV}$ [13], amplitude of light $A_0 = 3.8 \times 10^{12} \text{ eV} \cdot \text{s/C} \cdot m$, the band gap $\Delta = 1.16 \text{ eV}$, and the spin-orbit coupling strength $\lambda = 75 \text{ meV}$.

where we use the notations $\cos \theta_{s,\eta} = (\Delta - s\lambda\eta)/2E_{s,\eta}(\mathbf{p})$ and $\sin \theta_{s,\eta} = \eta vp/E_{s,\eta}(\mathbf{p})$ with the conduction band electron energy $E_c(\mathbf{p}) = s\eta\lambda/2 + E_{s,\eta}(\mathbf{p})$, $E_{s,\eta}(\mathbf{p}) = \sqrt{(vp)^2 + [(\Delta - s\lambda\eta)/2]^2}$. Since the transitions from the impurity state with a given valley number η to the conduction band of the other valley $\eta' \neq \eta$ are strongly suppressed due to the large distance between the valleys in the reciprocal space [12], the main contribution to the light absorption comes from the impurity-band transitions with the same valley number $\eta' = \eta$. From the point of view of applications, the most interesting is the circularly-polarized EM field case. The Hamiltonian describing the interaction of electrons with the external EM perturbation reads $\hat{V}(r, t) = -e\mathbf{v} \cdot \mathbf{A}(\mathbf{r}, t)$, where $\mathbf{A}(\mathbf{r}, t) = \mathbf{A}_0 \exp(i\mathbf{k}\mathbf{r} - i\omega t) + \mathbf{A}_0^* \exp(-i\mathbf{k}\mathbf{r} + i\omega t)$ is the vector potential of EM field, with \mathbf{k} and ω being the photon wave vector and frequency, correspondingly.

Electric current density. The general expression for the (partial) component of photon-drag electric current density, corresponding to electron transition from the impurity state with a quantum number m to the conduction band, reads ($\alpha = x, y$)

$$j_{m\alpha} = \frac{2\pi en_i \tau}{\hbar} \int \frac{v_\alpha(\mathbf{p}) d\mathbf{p}}{(2\pi\hbar)^2} |M_m(\mathbf{p}, \mathbf{k})|^2 \delta(E_c(\mathbf{p}) - E_i - \hbar\omega), \quad (13)$$

where n_i is the impurity concentration, e is the elementary charge, τ is the electron relaxation time in conduction band, $M_m(\mathbf{p}, \mathbf{k}) = \langle \psi_{s,\eta}(\mathbf{p}) | \hat{V} | \chi_{s,m}(\mathbf{p} - \mathbf{k}) \rangle$

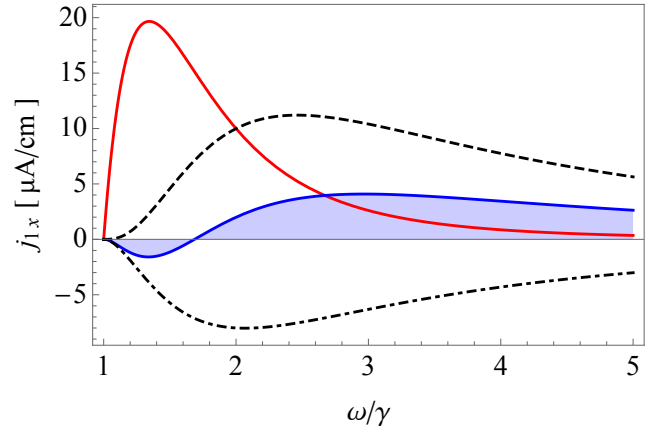


FIG. 3. Spectrum of electric current density due to the transitions from $m = 1$, $\eta = -1$ impurity states to spin-up conduction band states for the polarizations of light $\sigma = -1$ (red) and $\sigma = 1$ (blue); $\gamma = \epsilon_{1,1,-1}^i/\hbar$. The other parameters are taken the same as in Fig. 2.

is the matrix element of impurity-band transitions, and the electron velocity components are $v_x(\mathbf{p}) = \eta \sin \theta_{\mathbf{p}} \cos \varphi_{\mathbf{p}}$; $v_y(\mathbf{p}) = -i\eta \sin \theta_{\mathbf{p}} \sin \varphi_{\mathbf{p}}$. $E_i = \Delta/2 - \epsilon_{s,m,\eta}^i$ is the impurity energy level. Considering the $m = 0$ impurity state, we find the corresponding matrix element,

$$|M_0(\mathbf{p}, \mathbf{k})|^2 = (evA_0)^2 (\hbar v)^2 \frac{2\pi \epsilon_{s,0,\eta}^i}{\Delta} \times \left\{ \frac{(\eta + \sigma)^2 v^2 (\mathbf{p} - \mathbf{k})^2 \cos^2 \left(\frac{\theta_{s,\eta}}{2} \right)}{\left[v^2 (\mathbf{p} - \mathbf{k})^2 + \epsilon_{s,0,\eta}^i (\Delta - s\lambda\eta) \right]^2} + \frac{(\eta - \sigma)^2 (\Delta - s\lambda\eta)^2 \sin^2 \left(\frac{\theta_{s,\eta}}{2} \right)}{\left[v^2 (\mathbf{p} - \mathbf{k})^2 + \epsilon_{s,0,\eta}^i (\Delta - s\lambda\eta) \right]^2} \right\}. \quad (14)$$

Without the loss of generality, let us choose \mathbf{k} to be directed along the x-axis. Then, in Eq. (13) only the term containing $\cos \varphi_{\mathbf{p}}$ survives and $j_y = 0$, that reflects the fact that the photon-drag current should be directed along the photon wave vector. Substituting Eq. (14) in Eq. (13), we find

$$j_{0x} = \beta'_0 \Theta[\delta\hbar\omega_{s,0,\eta}] \frac{k\pi}{v} \frac{(\Delta - s\lambda\eta) + \delta\hbar\omega_{s,0,\eta}}{\left[(\delta\hbar\omega_{s,0,\eta})^2 + (\Delta - s\lambda\eta)\hbar\omega \right]^2} \times \frac{\delta\hbar\omega_{s,0,\eta}}{(\Delta - s\lambda\eta) + \delta\hbar\omega_{s,0,\eta}} \left\{ \frac{4(\Delta - s\lambda\eta)^2}{(\delta\hbar\omega_{s,0,\eta})^2 + (\Delta - s\lambda\eta)\hbar\omega} \times \delta\hbar\omega_{s,0,\eta}(\eta - \sigma)^2 + \left[(\Delta - s\lambda\eta) + \delta\hbar\omega_{s,0,\eta} \right] (\eta + \sigma)^2 \right. \\ \left. \times \left[\frac{4 \left((\Delta - s\lambda\eta) + \delta\hbar\omega_{s,0,\eta} \right) \delta\hbar\omega_{s,0,\eta}}{(\delta\hbar\omega_{s,0,\eta})^2 + (\Delta - s\lambda\eta)\hbar\omega} - 2 \right] \right\}, \quad (15)$$

where $\beta'_0 = en_i \tau v^2 \epsilon_i (evA_0)^2 / \hbar \Delta$ and $\delta \hbar \omega_{s,m,\eta} = \hbar \omega - \epsilon_{s,m,\eta}^i$. Figure 2 shows the spectrum of electric current density for different polarizations of light and $m = 0$, $\eta = -1$. Interesting to note, that in the case of the polarization of light $\sigma = -1$, the electric current flows in the opposite direction in some region of frequencies and then it changes its direction. Mathematically, it happens due to an interplay of different terms in Eq. (15), shown as dashed curves. Such behavior is not observed for $\sigma = 1$. For the case $m = 1$ (and, correspondingly, $\eta = -1$), we find

$$|M_1(\mathbf{p}, \mathbf{k})|^2 = (evA_0)^2 (\hbar v)^2 \frac{2\pi(\Delta^2 - \lambda^2)}{\Delta \epsilon_{s,1,-1}^i} \quad (16)$$

$$\times \left\{ \frac{(\sigma - 1)^2 (\epsilon_{s,1,-1}^i)^2 \cos^2 \left(\frac{\theta_{s,-1}}{2} \right)}{\left[v^2 (\mathbf{p} - \mathbf{k})^2 + \epsilon_{s,1,-1}^i (\Delta + s\lambda) \right]^2} + \frac{(\sigma + 1)^2 v^2 (\mathbf{p} - \mathbf{k})^2 \sin^2 \left(\frac{\theta_{s,-1}}{2} \right)}{\left[v^2 (\mathbf{p} - \mathbf{k})^2 + \epsilon_{s,1,-1}^i (\Delta + s\lambda) \right]^2} \right\}.$$

Again, only the x-component of the current is finite,

$$j_{1x} = \beta'_1 \Theta[\delta \hbar \omega_{s,1,-1}] \frac{k\pi}{v} \frac{(\Delta + s\lambda) + \delta \hbar \omega_{s,1,-1}}{\left((\delta \hbar \omega_{s,1,-1})^2 + (\Delta + s\lambda) \hbar \omega \right)^2}$$

$$\times \frac{\delta \hbar \omega_{s,1,-1}}{(\Delta + s\lambda) + 2\delta \hbar \omega_{s,1,-1}} \left\{ \frac{(\Delta + s\lambda) + \delta \hbar \omega_{s,1,-1}}{(\delta \hbar \omega_{s,1,-1})^2 + (\Delta + s\lambda) \hbar \omega} \right.$$

$$\times 4(\epsilon_{s,1,-1}^i)^2 (\sigma - 1)^2 + \delta \hbar \omega_{s,1,-1} (\sigma + 1)^2$$

$$\left. \times \left(\frac{4((\Delta + s\lambda) + \delta \hbar \omega_{s,1,-1}) \delta \hbar \omega_{s,1,-1}}{(\delta \hbar \omega_{s,1,-1})^2 + (\Delta + s\lambda) \hbar \omega} - 2 \right) \right\}, \quad (17)$$

where $\beta'_1 = \beta'_0 [\Delta^2 - \lambda^2] / \epsilon_i^2$. Figure 3 shows the spectrum of electric current density for $m = 1$. We choose $\eta = -1$ since for $\eta = 1$ the current is zero here (compare with Fig. 2). Also, it is the $\sigma = 1$ polarization which gives the region of positive and negative electric currents (blue curve). For a given σ , we have optical transitions in both the K (for $m = 0$ or 1) and K' (for $m = 1$ or 0) valleys. They can sum up or partially compensate each other.

Light absorption coefficient. Furthermore, let us study the light absorption coefficient for the m -th impurity state. It is defined as the ratio of the energy flux of absorbed photons and the average energy flux of incident photons [14], $\alpha_m(\hbar \omega) = \hbar \omega W_m / P$, where P is the average of the Poynting flux for the light intensity [15], $P = n_r c \epsilon_0 \omega^2 A_0^2 / 2$, where n_r is the refractive index of MoS₂ and ϵ_0 is the vacuum permittivity. The probability of light absorption in a given valley η and from a particular impurity state m is given by the Fermi golden rule,

$$W_m(\omega) = \frac{2\pi n_i}{\hbar} \int \frac{d\mathbf{p}}{(2\pi\hbar)^2} |M_m(\mathbf{p}, 0)|^2 \delta(E_c(\mathbf{p}) - E_i - \hbar \omega).$$

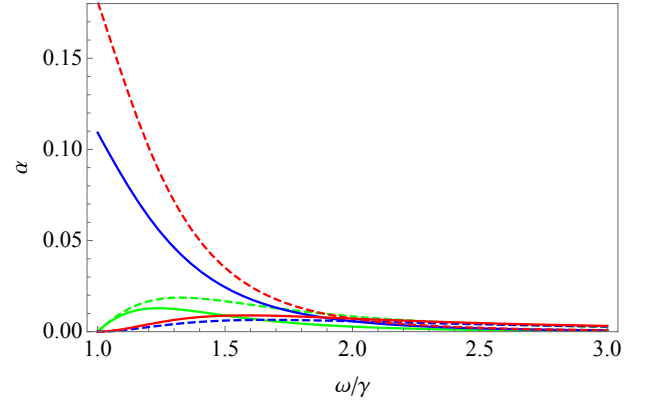


FIG. 4. Spectrum of absorbance for $m = 0$ (solid) and $m = 1$ (dashed) and $\sigma = -1$ (red) and $\sigma = 1$ (blue). (Inset) Schematic band structure of MoS₂.

For the transition from $m = 0$ impurity state, we find

$$\alpha_0 = \frac{2\pi n_i e^2 v^2 \epsilon_{s,0,\eta}^i \Theta[\delta \hbar \omega_{s,0,\eta}] \delta \hbar \omega_{s,0,\eta}}{n_r c \omega \Delta \epsilon_0 (\Delta - s\lambda\eta) + 2\delta \hbar \omega_{s,0,\eta}}$$

$$\times \frac{\sqrt{4(\Delta - s\lambda\eta + \delta \hbar \omega_{s,0,\eta}) \delta \hbar \omega_{s,0,\eta} + (\Delta - s\lambda\eta)^2}}{\left((\delta \hbar \omega_{s,0,\eta})^2 + (\Delta - s\lambda\eta - \epsilon_{s,0,\eta}^i) \hbar \omega \right)^2}$$

$$\times \left\{ (\eta + \sigma)^2 (\Delta - s\lambda\eta + \delta \hbar \omega_{s,0,\eta})^2 + (\eta - \sigma)^2 (\Delta - s\lambda\eta)^2 \right\},$$

and for $m = 1, \eta = -1$ state,

$$\alpha_1 = \frac{2\pi n_i e^2 v^2 \Theta[\delta \hbar \omega_{s,1,-1}] \Delta^2 - \lambda^2}{n_r c \omega \Delta \epsilon_0 \epsilon_{s,1,-1}^i} \frac{(\Delta + s\lambda) + \delta \hbar \omega_{s,1,-1}}{(\Delta + s\lambda) + 2\delta \hbar \omega_{s,1,-1}}$$

$$\times \frac{\sqrt{4(\Delta + s\lambda + \delta \hbar \omega_{s,1,-1}) \delta \hbar \omega_{s,1,-1} + (\Delta + s\lambda)^2}}{\left((\delta \hbar \omega_{s,1,-1})^2 + (\Delta + s\lambda - \epsilon_{s,1,-1}^i) \hbar \omega \right)^2}$$

$$\times \left\{ (\sigma - 1)^2 (\epsilon_{s,1,-1}^i)^2 + (\sigma + 1)^2 (\delta \hbar \omega_{s,1,-1})^2 \right\}. \quad (18)$$

Figure 4 shows the spectra of absorbance. For the transitions from the state $m = 1$, the magnitude of absorbance is higher for the $\sigma = -1$ light but by increasing the photon energy, the valley dependence disappears. For the transitions from the state $m = 0$, both the polarized lights give comparable contribution.

It is enlightening to compare the matrix element corresponding to impurity-band transitions with the matrix element for the interband transitions, $|M_{cv}(p)|^2$ [5]. The valley selectivity for interband transitions is to a large extent satisfied only at small values of momentum p , giving $|M_{cv}(0)|^2 \propto (\eta + \sigma)^2$. In our case, the transitions from $m = 0$ impurity states are strongly suppressed due to $|M_0(0,0)|^2 \rightarrow 0$, whereas for $m = \pm 1$

we find $|M_{m=\pm 1}(0,0)|^2 \propto \epsilon_i^2(\sigma + \eta)^2$ under the condition $m + \eta = 0$. It means that the valley selectivity takes place for orbital impurity states $m = \pm 1$ (and thus we have $\exp(im\varphi) \neq 1$), reflecting the chirality of the band electron wavefunction. These general conclusions are supported by the numerical analysis. For instance, the absorption coefficient in Fig. 4 is large in the vicinity of the threshold for $m = 1, \eta = -1$ state at $\sigma = -1$ polarization.

In conclusion, we have studied the selection rules for the light-induced transitions from impurity states to the conduction band in two-dimensional gapped Dirac ma-

terials. For that, we calculated and investigated the absorption coefficient and the photon-drag-induced electric current. For clarity, we used the shallow impurity potential model. Nevertheless, this model correctly reflects the selection rules of any impurity possessing the azimuthal symmetry. Thus, our conclusions on the optical selection rules are sufficiently general.

Acknowledgements. We thank M. Sun and I. Vakulchyk for useful discussions. We acknowledge the support by the Institute for Basic Science in Korea (Project IBS-R024-D1) and the Russian Science Foundation (Project 17-12-01039).

-
- [1] D. Xiao, W. Yao, and Q. Niu, Valley-contrasting physics in graphene: Magnetic moment and topological transport, *Phys. Rev. Lett.* **99**, 236809 (2007).
 - [2] D. Xiao, G.-B. Liu, W. Feng, X. Xu, and W. Yao, Coupled spin and valley physics in monolayers of MoS_2 and other group-vi dichalcogenides, *Phys. Rev. Lett.* **108**, 196802 (2012).
 - [3] Z. M. Wang, *MoS2: materials, physics, and devices* (Springer, Cham, Switzerland, 2014).
 - [4] J. Silva-Guillén, P. San-Jose, and R. Roldán, Electronic band structure of transition metal dichalcogenides from ab initio and slater-koster tight-binding model, *Applied Sciences* **6**, 284 (2016).
 - [5] V. M. Kovalev, W.-K. Tse, M. V. Fistul, and I. G. Savenko, Valley hall transport of photon-dressed quasiparticles in two-dimensional dirac semiconductors, *New Journal of Physics* **20**, 083007 (2018).
 - [6] H. Zeng, J. Dai, W. Yao, D. Xiao, and X. Cui, Valley polarization in MoS_2 monolayers by optical pumping, *Nature Nanotech.* **7**, 490 (2012).
 - [7] S. S. Li, Optical properties and photoelectric effects, in *Semiconductor Physical Electronics* (Springer US, Boston, MA, 1993) Chap. 9, pp. 246–283.
 - [8] S. Refaely-Abramson, D. Y. Qiu, S. G. Louie, and J. B. Neaton, Defect-induced modification of low-lying excitons and valley selectivity in monolayer transition metal dichalcogenides, *Phys. Rev. Lett.* **121**, 167402 (2018).
 - [9] V. Tulupenko, A. Abramov, Y. Belichenko, V. Akimov, T. Bogdanova, V. Poroshin, and O. Fomina, The influence of the ionized impurity delta-layer potential in the quantum well on impurity binding energy, *Journal of Applied Physics* **109**, 064303 (2011).
 - [10] A. V. Chaplik and L. I. Magarill, Bound states in a two-dimensional short range potential induced by the spin-orbit interaction, *Phys. Rev. Lett.* **96**, 126402 (2006).
 - [11] A. Pakhomov, K. Khalipov, and I. Yassievich, Local electronic states in semiconductor quantum wells, *Semiconductors* **30**, 730 (1996).
 - [12] M. Goryca, N. P. Wilson, P. Dey, X. Xu, and S. A. Crooker, Detection of thermodynamic “valley noise” in monolayer semiconductors: Access to intrinsic valley relaxation time scales, *Science Advances* **5**, eaau4899 (2019).
 - [13] H. Hatami, T. Kernreiter, and U. Zülicke, Spin susceptibility of two-dimensional transition-metal dichalcogenides, *Physical Review B* **90**, 045412 (2014).
 - [14] H. Fang, H. A. Bechtel, E. Plis, M. C. Martin, S. Krishna, E. Yablonovitch, and A. Javey, Quantum of optical absorption in two-dimensional semiconductors, *PNAS* **110**, 11688 (2013).
 - [15] S. L. Chuang, *Physics of photonic devices*, Vol. 80 (John Wiley & Sons, Hoboken, New Jersey, 2012).